In-situ Micro-thermography Reveals Inverse Relationship Between Ice Nucleation and Ice Growth in Frozen Foods

Martin Zalazar[1,2], Shriya Jitendra Kalburge[3], Yining Zhang[3] and Ran Drori[1,3]

[1]Department of Chemistry and Biochemistry, Yeshiva University, 245 Lexington Avenue, New York, NY 10016
[2]Instituto de Investigación y Desarrollo en Bioingeniería y Bioinformática (CONICET-UNER) and Facultad de Ingeniería, Universidad Nacional de Entre Ríos, Ruta Prov. 11 (Km 10), (3100) Oro Verde, Entre Ríos, Argentina.
[3]Biothechnology Management and Entrepreneurship, Katz School of Science and Health, Yeshiva University, 215 Lexington Avenue, New York, NY 10016

Abstract

According to a USDA report, $161 billion worth of food products was not available for human consumption in 2010 due to food loss. One potential way to reduce food loss is to prevent damage during the freezing process. This study presents quantitative measurements of the two primary processes involved in freezing: ice nucleation and ice growth. Using a newly developed micro-thermography system, we measured in-situ rates of ice nucleation and growth. Our findings indicate that ice nucleation and ice growth are distinct and opposing processes. Specifically, ice nucleation rates in beef and zucchini were significantly higher than those in broccoli and potato, whereas ice growth was faster in broccoli and potato compared to beef and zucchini. Analyzing the chemical composition of these foods enables the application of established crystal growth principles on freezing of foods. Therefore, designing a customized freezing process for each food product will lead to improved quality.

Introduction

The freezing process of food products is designed to extend shelf life while limiting nutrient and sensory damage to the product caused by ice. This process includes two main stages: ice nucleation (or formation of ice) followed by ice crystal growth[1]. Ice nucleation is a process within which small ice nuclei form in a supercooled environment, and grow to become ice crystals with the assistance of surfaces (heterogenous nucleation) or without this assistance (homogenous nucleation)[2]. Supercooling refers to the phenomenon where a liquid is cooled below its freezing point without undergoing a phase transition to the solid state. In the context of freezing processes, it is the extent to which a liquid is cooled below its freezing point before nucleation and subsequent ice crystal growth occur. Ice growth is the expansion of existing ice crystals by the addition of water molecules from the surrounding liquid to the ice lattice. The literature of frozen foods describes ice nucleation temperatures (or freezing point) of each food type (meat, fruit, vegetable etc.) as a range of temperatures[3–9] measured using thermistors in the food product[4], firmness change[5] and calorimetric estimation of the freezing point[9]. However, ice nucleation is a stochastic process, which is affected by many factors such as cooling rates and time spent at freezing temperatures, thermal conductivity of the cooling element and the sample, as well as size and shape of the sample. These varying factors might provide false values of freezing temperature, and the obtained values might be method and sample specific. Quantifying the rate of ice nucleation in food products will provide more accurate and quantitative data that will eliminate the elusive factors mentioned above. Coupling the measurement of ice nucleation rate to ice growth velocity would provide a holistic understanding of the freezing process of foods.

Recently, we described a new micro-thermography system developed in our lab, and designed to measure ice growth velocity and ice nucleation rates in-situ in non-transparent sample, specifically in food[10]. Here, this system was used to elucidate the freezing process of various food products, by measuring both ice growth velocity and ice nucleation rates. We found that ice nucleation and ice growth in food products are two distinct processes within the freezing process and that these processes can operate in opposing directions.

Methods

Temperature control and thermal imaging systems

A system comprising a cold stage coupled with a thermal camera described previously[10], was used for the ice growth velocity experiments. In short, the system included a temperature controller (586 series TECPak, Arroyo Instruments, San Luis Obispo, CA) that governs the temperature of the copper cold stage via Peltier thermoelectric coolers and a thermistor, which is inserted into the copper cold stage. The copper cold stage is housed in an acrylic box with an aluminum lid (to prevent condensation) with a germanium window. A high-resolution (2048 x 1536 IR px) thermal camera (VarioCAM® HD head 800 with Micro-scanning upgrade, InfraTec GmbH, Germany) was used and its accuracy was ensured by calibrating it against various sample temperatures[10].

For the ice nucleation experiments, a portable thermal camera (T3 Pro, Yantai, China) with a resolution of 384x288 IR px was used, and a cold stage (similar to the one described above) was constructed to obtain the Food Ice Nucleation Assay (FINA). The thermal camera was connected to an Android tablet for image acquisition, and the temperature of the cold stage was governed by a temperature controller (585 series TECPak, Arroyo Instruments, San Luis Obispo, CA). A LabVIEW program was developed to control the temperature of the cold stage.

Ice growth velocity and nucleation rate measurements

In addition to data acquisition, a series of essential post-processing steps were implemented to measure growth velocities and nucleation rates, and analyze related data, ensuring precision and facilitating effective data interpretation.

Sample Preparation

In the sample preparation process, thin layers were obtained from the selected sample (e.g., a potato cube) using a hand-held microtome with a razor knife. These thin layers were then shaped to the desired diameter using a sharp cutting tool. The organized placement of these samples on a copper plate atop the cold stage, facilitated by a plastic grid, set the groundwork for subsequent experiments. The utilization of a low-thermal-conductivity plastic grid serves to mitigate temperature variations caused by potential misplacement of samples on the copper plate and minimizes the impact of neighboring effects[i] resulting from heat release.

Frame analysis and data file generation

For the growth rate study, the camera was employed to capture sequences of frames during the experimental process, which provided critical information for subsequent analysis. In the initial post-processing phase, IRbis software played a vital role in data extraction and preparation. This encompassed a frame selection, where three frames were strategically chosen to represent distinct phases of ice growth: initiation, termination, and an intermediate stage. Additionally, the software was employed for melting point identification by analyzing the temperature profile, recognizing a

well-defined trough as the melting point and a flat profile signaled this event. The identification of the melting point was described visually in reference[10].

Temperature profiles were established through the placement of measurement lines from the initiation of ice growth to the conclusion of crystal growth, accompanied by reference rectangles (Fig S1). Importantly, these reference rectangles were used for measuring the temperature of the unfrozen regions during ice growth. The collected data, including temperature profiles and measurement line details, were cataloged in spreadsheets. Furthermore, the software was employed to process the temperature profile data and generate a profile time chart, subsequently exporting it in text format for further analysis. For the second post-processing stage, an app was built by using the "App Designer" tool of Matlab™ software, to optimize a sequence of tasks. First, data loading was executed by importing the experiment data, including distinct temperature cooling slopes and corresponding frame numbers (Fr1, Fr2, Fr3) and temperatures (T1, T2, T3) (Fig S1). Additionally, the melting temperature was defined for reference. Subsequently, graph plotting was initiated to visualize the data and calculate growth rates (GR). To refine the curves and enhance GR calculations, the "Smoothing" function was applied. To ensure precise calculations, the "Threshold" function was utilized to pinpoint the start and end temperature points, contributing to accurate assessments of both growth rates and temperature differences (DT). The processed results were systematically stored in text files via the "Calc" function, following a predefined format to facilitate reference and analysis. For rapid, convenient visual representation of outcomes, the "Load & Plot GR File" button was harnessed, enabling the visualization of data and analysis results.

Food Ice Nucleation Assay (FINA) data recording and postprocessing

Temperature data control and recording were managed using a LabVIEW as described before[10]. To identify and record nucleation events, a video editing software (Nikon NIS-Elements, U.S.A) was employed to select nucleation samples and extract their parameters. This was followed by the utilization of a Matlab™ application to determine both the temperature and timing of the nucleation events. Moreover, this software tool facilitated the generation of graphical representations depicting the response of chosen events, specifically in terms of mean intensity over time (see Fig. S2).

Calculation of Ice nucleation Rate

The ice nucleation rate calculation was obtained by analyzing nucleation temperature data and the measured contact area of the samples, as used in elsewhere[11,12]. The nucleation rate (J) is expressed as:

Eq. 1 $$J = \frac{N_f^i}{\frac{\Delta T}{c}\left(N^i_{unfr-N_f^i}\right)+\sum_{j=1}^{N_f^i}\Delta t_{f,j}}$$

Where N_f^i is the number of frozen samples in each temperature interval, denoted as the i[th] interval. ΔT represents the width of the temperature interval (typically 0.5-1 °C), c is the cooling rate, N_{unfr}^i is the number of unfrozen samples at the beginning of the interval, and $\Delta t_{f,j}$ represents the time it took for the j[th] sample to freeze within that interval. The obtained rate (J) was normalized by the area of the sample (A), which was typically 7 mm^2.

Eq. 2 $$R = \frac{J}{A}$$

Thus, the nucleation rate coefficient, R, is expressed in terms of number of nucleation events per time per area. These calculations enable the determination of the nucleation rate in a comprehensive manner, even in cases with changing temperatures, providing valuable insights into the freezing behavior of the samples.

Results and Discussion

Ice nucleation rates inside food products using FINA

When a food product is placed at sub-freezing temperature, ice nucleation is the first step towards freezing the whole product. After ice is formed (nucleated), the newly formed crystals grow inside the food at a velocity proportional to the supercooling degree. The rates in which ice nucleation occur in various food products were measured in terms of number of nucleation events per area per time, which is different compared to other studies that determined the temperatures in which the studied samples froze[3–5,13,14]. Here, the samples were cooled to 0 ºC at 0.5 ºC/sec, and then the cooling rate was slowed down to 1 ºC/min. The cooling process continued until all samples froze (~-20 ºC), while the thermal camera was recording (see video snapshot in Fig. 1A). The output video was analyzed (see more details in the experimental section) and nucleation rates were obtained for each type of food sample (beef, broccoli, zucchini and potato). To fit the experimental data for the ice nucleation rate, R, a classical nucleation theory (CNT) from Cabriolu *et al.*[15] was used.

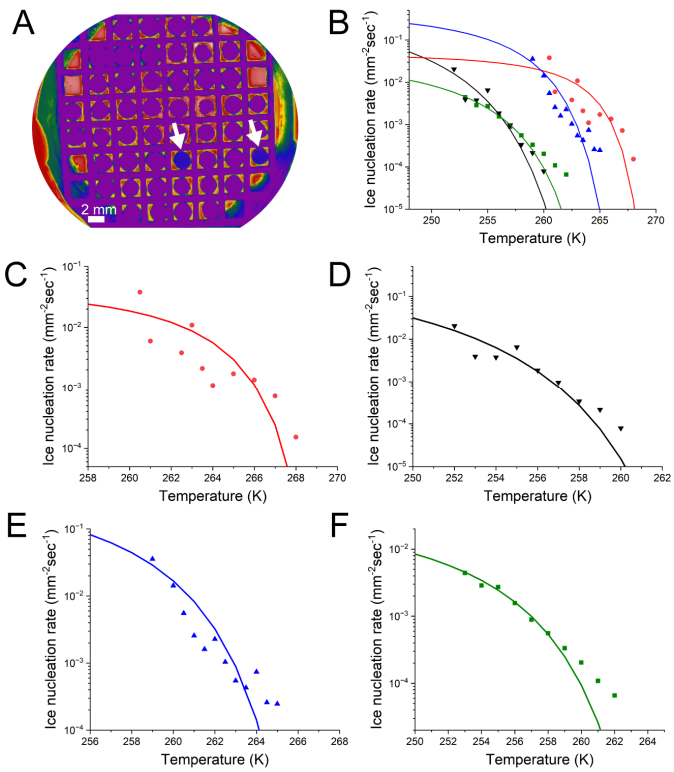

Fig. 1. Array of samples in the FINA system (A). The blue color indicates the release of latent heat during nucleation events, also indicated by white arrows. Ice nucleation rates of all tested samples (B), as calculated using the formula detailed above. Ice nucleation rates for beef (C), potato (D), zucchini (E) and broccoli (F). The absolute temperature is presented in K for simplicity. The number of individual samples used for the nucleation experiments are 170, 61, 92 and 166 for broccoli, beef, zucchini and potato, respectively.

Eq. 3
$$\ln(R) = \ln(A) + \frac{C}{(T-T_m)^2 T}$$

Where A and C are constants; A is a kinetic pre-factor and C expresses a temperature-dependent constant[15].

The obtained nucleation rates of all samples increased with the decrease of the temperature, as expected, and exhibited a reasonably good fit with classical nucleation theory[15] for heterogenous nucleation. Fig. 1B presents the nucleation rates of the tested food products vs. the absolute temperature (K). The results provide a hierarchy of ice nucleation probability in the tested food products, where ice nucleation rates were measured at much higher temperatures (268-260K) in

beef compared to broccoli and potato (262K-252K). The nucleation rates in zucchini were found to be closer to the rates measured in beef, and the rates measured in potato and broccoli are comparable and much lower than beef and zucchini. For example, the nucleation rate at 260K in beef is faster than the rate measured in potato and broccoli by 3 orders of magnitude. While the broccoli and potato samples were freezing at a temperature range of 262K-252K, the beef samples were completely frozen at 260K, and no rates were documented below that temperature. The nucleation rates measured here can be used to calculate the number of nucleation events in larger samples used in this study. For example, the number of nucleation events in a 2D piece of beef sized 10 cm^2 to -5 ºC (268K) is 5.3 per second. Decreasing the temperature to -13 ºC (260K) will increase the number of nucleation events to 1327.6 per second. A comparison of this value in beef to similarly sized samples of potato or broccoli at the same temperature shows the stark difference between the samples; the number of nucleation events is 2.7 and 7.1 per second, respectively.
These results provide useful information for calculating the number of nucleation events in a sample during cooling, and combined with our ice growth velocity measurements, the freezing procedure of food products can be improved. Furthermore, our ice nucleation data is very useful for developing the supercooling approach of food preservation[16], where ice formation is avoided.

Ice growth velocities inside food products

The growth velocities of ice crystals inside food products were measured by first freezing the samples completely, then melting most of the ice inside the sample to obtain a ratio of 1:5 frozen to unfrozen regions (Fig. S1). At this point, the temperature decreased at a constant rate and the ice progressed in the sample until the whole sample was frozen again. The experiment was performed using various cooling rates resulting in different supercooling degrees. One of the benefits of using a thermal camera for crystal growth velocity measurements is the ability to measure the temperature of the unfrozen regions of the sample in each frame, regardless of the cold stage's thermistor reading. Thus, a "live" reference temperature was used to calculate the supercooling degree by averaging the measured temperature in the unfrozen region in each recorded frame. The difference between the melting temperature of each sample and the reference temperature was defined as the supercooling degree. However, the measured temperature by the thermal camera mainly reflects the upper part of the sample, and a temperature gradient exists where the bottom part of the sample is colder than the upper part. Thus, COMSOL simulations were performed to quantify the temperature gradient at

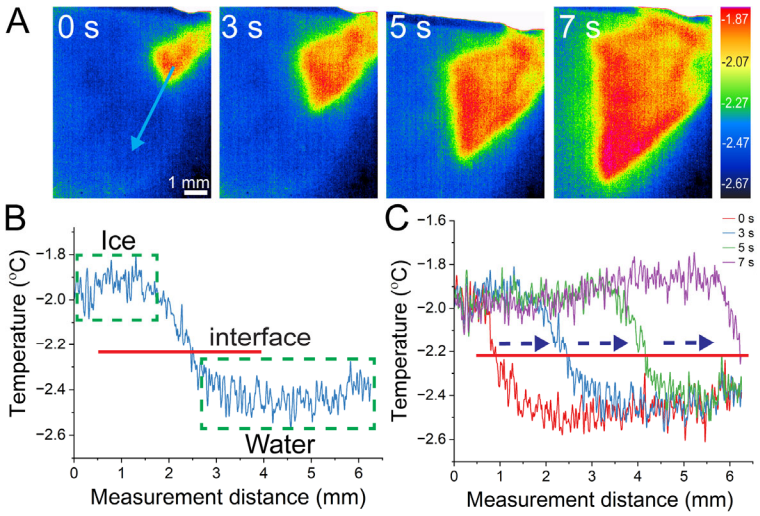

Fig. 2. A series of snapshots of an ice crystal growing inside broccoli stems as imaged by the thermal camera (A). The blue arrow in A was used as a temperature probe and the spatial temperature profile was plotted to identify the ice/water interface (B), which was then used to calculate the ice growth velocity by plotting the data from all snapshots (C).

fixed and changing temperatures. These simulations are presented in the SI and show the temperature distribution along the z-axis (vertical) within a biological sample (myocardium at 1 mm thickness) compared to the temperature of the copper cold stage (Fig. S3). As expected, the temperature within the myocardium increases with increased distance from the copper plate, which was held at -0.215 ºC during the simulation. However, the temperature increase is 13% at the most outer layer (furthest away from the cold stage) of the sample. The simulation shows that the largest temperature error in our growth velocity measurements is ~1.8 ºC at the highest supercooling measured (ΔT=14 ºC). A different simulation compared the temperature of the outer layer of the myocardium during cooling at 0.2 ºC/min, and the simulation data was compared to the temperature of a biological sample (apple) measured by the thermal camera during cooling at the same rate (Fig. S4).

The obtained results of the ice growth velocity experiments were clustered based on similar velocities, which also have some structural similarities. The experimental data was fitted by a double exponent formula. The velocities obtained in beef and chicken (Fig. 3A) were much slower than the velocities in broccoli and potato (Fig. 3B). Ice growth velocities in these food products exhibited similar values at low supercooling, but at higher supercooling (ΔT >8 ºC), ice grew slower in the chicken samples. Except in potato, the increase in growth velocity for beef, chicken and broccoli seemed to slow down at the highest supercooling measured (ΔT≈13 ºC). This behavior was also observed for other samples, such as apple and zucchini (Fig. 3C), in which a decreased velocity was measured at higher supercooling. As any crystal that grows in its melt, ice growth velocity should reach a maximum and slow down at higher supercooling. The supercooling degree in which a maximum growth velocity is observed for ice growing in pure water is still under debate[17–20]. The growth velocity measured in potato did not slow down at higher supercooling of 10 ºC, which contrasts with the velocity measured in broccoli (Fig. 3B). The slowest ice growth velocities were measured in dough and aqueous solutions containing 20% sucrose (Fig. 3D), which were slower than the velocities measured in potato and broccoli by a factor of 10 at the deep supercooling degrees (8-10 ºC). Thus, the range of velocities measured here was broad, and expanded from a few mm/sec to almost 50 mm/sec at the highest supercooling degrees (ΔT≈13 ºC). These large differences are presented in Fig. 4 for potato, beef, and dough. The water content was measured in each type of food product by dehydration in the oven for 360-480 minutes at 70 ºC and were found to be comparable to the values in the USDA database

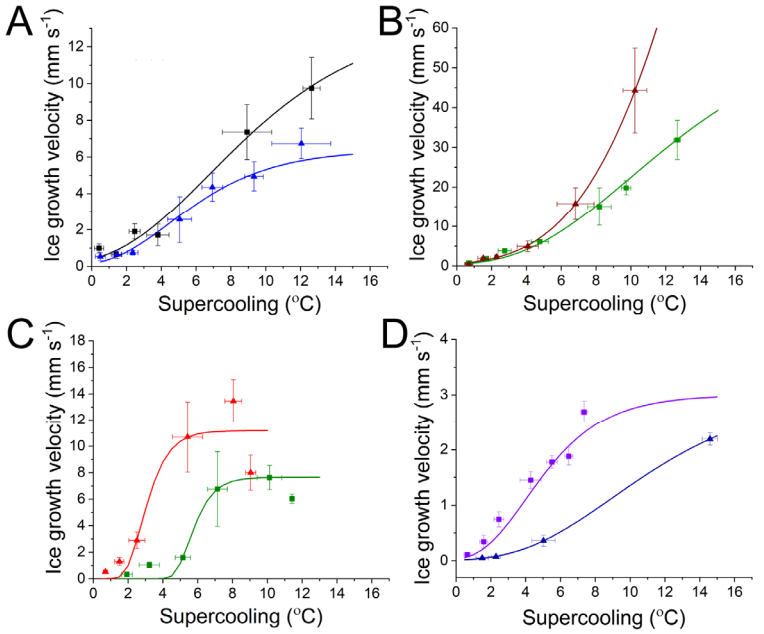

Fig. 3. Ice growth velocity in beef (black squares) and chicken (blue triangle) (A), potato (dark red triangles) and broccoli (green squares) (B), Zucchini (red triangles) and apple (green squares) (C), dough (purple squares) and 20% sucrose (dark blue triangles) (D).

(FoodData Central[21]). Factoring in the levels of sugars in each food provides an interesting interpretation of our results. The slowest growth velocity was measured in an aqueous solution containing 20% sucrose (thus, 80% water by weight), and the growth velocity in dough (45% water) was the second slowest. This finding indicates that low water content and high sugar content are implicated in slowing down ice growth velocity, which is well established in the literature[22,23]. As the ice front progresses, the local concentration of solutes (sugars, salts etc.) near the ice surface increases, which hinders the addition of water molecules from the liquid to the ice lattice[22,24]. The levels of mono and disaccharides in apple is higher (12%[21]) by almost a factor of 10 compared to the foods tested here, and ice growth velocity in apple was the slowest after dough, which has a much lower water content (85% in apple and 45% in dough). The slow ice growth velocity in beef and chicken may be attributed to low water content (60%) compared to the plant-based foods (81 – 95%), and the higher fat and protein content (13% fat and 27% proteins in beef compared to 0.05-0.32% fat and 0.17-2.57% proteins in plant-based foods). The highest ice growth velocity was measured in potato and broccoli, which have a high-water content (81 and 89%, respectively) and low levels of sugars (0.85 and 1.4, respectively), fat (0.05% in broccoli) and proteins (1.8 and 2.57%, respectively).

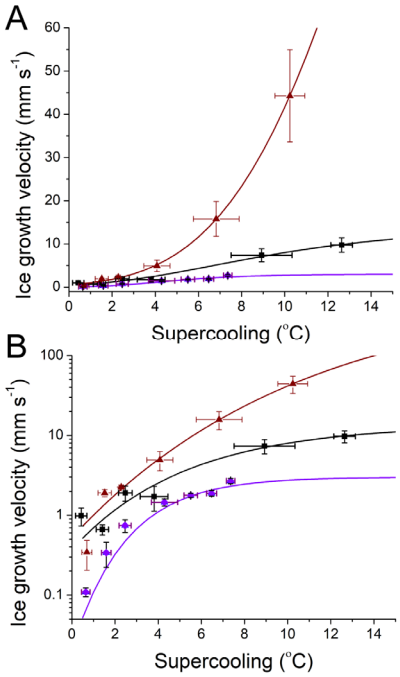

Fig. 4. Ice growth velocities in potato (green squares), beef (black squares) and dough (purple diamonds) in a linear scale (A) and in logarithmic scale (B).

These results indicate that ice growth velocity in fruits is much slower (up to a factor of 6 at ΔT=10 ºC) compared to vegetables, and the high sugar content is the main reason for the slower growth velocities.

To strengthen this notion, ice growth velocity in various sucrose concentrations were measured using light microscopy, and the nucleation temperature of each sucrose concentration was documented (see SI). The results of these measurements correspond well with our micro-thermography ice growth velocity measurements with 20% sucrose solutions. Ice growth velocity slowed down by 50-fold when sucrose concentration was increased from 2.5% to 40%. The ice nucleation temperatures of the sucrose solutions decreased with increased sucrose concentration; however, this effect was mild compared to the effect on growth velocities (Fig. S5).

Nucleation rates and growth velocity

To provide a holistic description of the freezing process of food products, the ice growth velocity and ice nucleation rates were plotted together for each of the tested food products (Fig. 5). These combined plots present the striking variance between samples. Ice grows slower in beef than in potato, broccoli and zucchini, however, faster ice nucleation rates were measured in beef compared to the other food products. Specifically, ice grows faster in potato than in beef by a factor of five (at ΔT=10 ºC), but ice nucleation occurs slower by two orders of magnitude compared to beef (at ΔT=12 ºC). The results also show that when comparing the different food products tested here, *ice growth velocity is inverted to ice nucleation rate*. In other words, zucchini and beef (Figs. 5A and 5B) freeze faster (more nucleation events at higher temperatures), but after the ice is formed, it

would grow much slower inside the product, compared to broccoli and potato. Figs. 5C and 5D provide the opposite effect for potato and broccoli, respectively, as these samples froze at higher supercooling degrees (ΔT=9-20 ºC) than beef and zucchini (ΔT=5-13 ºC). The finding that ice nucleation rates are faster compared to the rest of the tested food products may be related to ice nucleation of ferritin[25,26]. Ferritin is a 28 kDa protein that assembles in the cell into 24 subunits with an outer diameter of 12 nm[25] and can carry 4500 iron atoms. This protein is found in the cytoplasm and serum in mammals, and in plants they are located in the plastids[27], which might be less available to act as an ice nucleator. Nevertheless, proteins compose 27% of the mass of a beef product, while in plant-based foods tested here, the levels of proteins are much lower (1.21-2.57%[21]). The slow growth of ice in beef might be explained by the low water content (60%) compared to the plant-based foods (81-95%)[28] and the 2 orders of magnitude higher levels of fats (13% in beef compared to 0.05-0.32% in plants) that would inhibit ice growth by the same mechanism mentioned above for sugars. The results are presented in a schematic graph in Fig. 6.

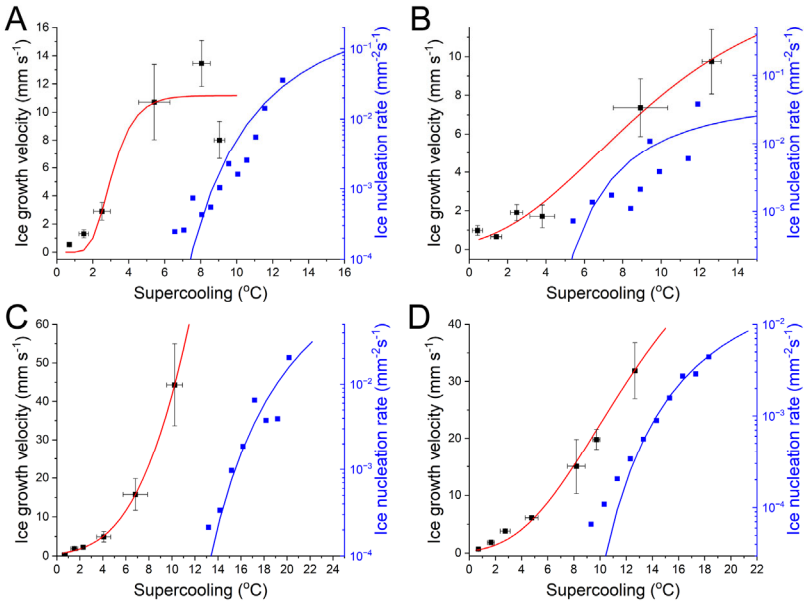

Fig. 5. Ice growth velocity and ice nucleation rates vs. supercooling in zucchini (A), beef (B), potato (C) and broccoli (D). The measured melting points of ice in zucchini, beef, potato and broccoli were -1.44, -0.58, -0.82 and -1.68 ºC, respectively.

Conclusions

In this study we elucidated the freezing process of various food products by measuring the rate at which ice is formed inside the food product (ice nucleation), and the velocity in which ice grows in the food product after formation of a crystal. We highlight here the importance of dynamic measurements such as ice nucleation rates and ice growth velocity, in understanding the freezing process inside food products. Our results clearly demonstrate that ice nucleation and ice growth are two distinct processes that operate independently and should be well understood to improve the quality of frozen foods. We measured *faster* ice nucleation rates in beef and zucchini compared to potato and broccoli, however, after the formation of ice, we found that its velocity was much faster in potato and broccoli. Thus, the specific composition of each food product (water content, levels of proteins, sugars, and fats), along with deep understanding of the freezing process will provide improved frozen food quality.

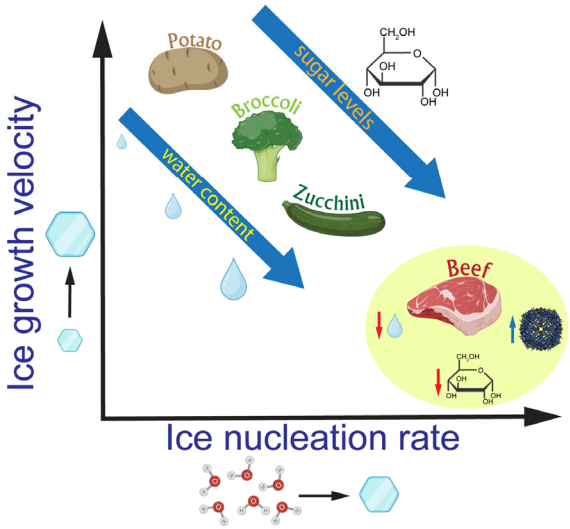

Fig. 6. An inverted correlation between ice nucleation rate and ice growth velocity was found for potato, broccoli, zucchini and beef samples. Parts of the figure were created with BioRender.com.

Acknowledgments

The authors acknowledge the generous support from the United States Department of Agriculture, National Institute of Food and Agriculture (Award No. 2022-67018-36539).

References

1. You, Y., Kang, T. & Jun, S. Control of Ice Nucleation for Subzero Food Preservation. *Food Eng. Rev.* **13**, 15–35 (2021).
2. Cantrell, W. & Heymsfield, A. Production of ice in tropospheric clouds: A review. *Bull. Am. Meteorol. Soc.* **86**, 795–807 (2005).
3. James, C., Hanser, P. & James, S. J. Super-cooling phenomena in fruits , vegetables and seafoods. *11th Int. Congr. Eng. Food (ICEF 2011)* 6–11 (2011).
4. James, C., Seignemartin, V. & James, S. J. The freezing and supercooling of garlic (Allium sativum L.). *Int. J. Refrig.* **32**, 253–260 (2009).
5. Fukuma, Y., Yamane, A., Itoh, T., Tsukamasa, Y. & Ando, M. Application of supercooling to long-term storage of fish meat. *Fish. Sci.* **78**, 451–461 (2012).
6. Osuga, R., Koide, S., Sakurai, M., Orikasa, T. & Uemura, M. Quality and microbial evaluation of fresh-cut apples during 10 days of supercooled storage. *Food Control* **126**, 108014 (2021).
7. Koide, S., Ito, T., Osuga, R. & Orikasa, T. Assessment of cumulative freezing frequency of supercooled fresh-cut onion: Effects of sample size, supercooling temperature, and supercooled storage time. *J. Agric. Food Res.* **10**, 100440 (2022).
8. Jeremiah, L. E. & Gibson, L. L. The influence of storage temperature and storage time on color stability, retail properties and case-life of retail-ready beef. *Food Res. Int.* **34**, 815–

826 (2001).
9. Rahman, M. S. *et al.* Analysis of cooling curve to determine the end point of freezing. *Food Hydrocoll.* **16**, 653–659 (2002).
10. Zalazar, M., Zypman, F. & Drori, R. Micro-thermography for imaging ice crystal growth and nucleation inside non-transparent materials. *Rev Sci Instrum* **94**, 054903 (2023).
11. Lata, N. N. *et al.* Multivalent Surface Cations Enhance Heterogeneous Freezing of Water on Muscovite Mica. *J. Phys. Chem. Lett.* **11**, 8682–8689 (2020).
12. Zobrist, B., Koop, T., Luo, B. P., Marcolli, C. & Peter, T. Heterogeneous ice nucleation rate coefficient of water droplets coated by a nonadecanol monolayer. *J. Phys. Chem. C* **111**, 2149–2155 (2007).
13. Sequeira-Munoz, A., Chevalier, D., Simpson, B. K., Le Bail, A. & Ramaswamy, H. S. Effect of pressure-shift freezing versus air-blast freezing of carp (Cyprinus carpio) fillets: A storage study. *J. Food Biochem.* **29**, 504–516 (2005).
14. Chen, Y. & Pan, B. S. Morphological changes in tilapia muscle following freezing by airblast and liquid nitrogen methods. 159–168 (1997) doi:10.1046/j.1365-2621.1997.00392.x.
15. Cabriolu, R. & Li, T. Ice nucleation on carbon surface supports the classical theory for heterogeneous nucleation. *Phys. Rev. E - Stat. Nonlinear, Soft Matter Phys.* **91**, 1–7 (2015).
16. Lin, H. *et al.* The importance of supercooled stability for food during supercooling preservation: a review of mechanisms, influencing factors, and control methods. *Crit. Rev. Food Sci. Nutr.* **0**, 1–15 (2023).
17. Buttersack, T. & Bauerecker, S. Critical Radius of Supercooled Water Droplets: On the Transition toward Dendritic Freezing. *J. Phys. Chem. B* **120**, 504–512 (2016).
18. Montero De Hijes, P., Espinosa, J. R., Vega, C. & Sanz, E. Ice growth rate: Temperature dependence and effect of heat dissipation. *J. Chem. Phys.* **151**, (2019).
19. Shibkov, A. A., Golovin, Y. I., Zheltov, M. A., Korolev, A. A. & Leonov, A. A. Morphology diagram of nonequilibrium patterns of ice crystals growing in supercooled water. *Phys. A Stat. Mech. its Appl.* **319**, 65–79 (2003).
20. Shibkov, A. A., Zheltov, M. A., Korolev, A. A., Kazakov, A. A. & Leonov, A. A. Crossover from diffusion-limited to kinetics-limited growth of ice crystals. *J. Cryst. Growth* **285**, 215–227 (2005).
21. USDA. FoodData Central. https://fdc.nal.usda.gov/fdc-app.html#/food-details/1103172/nutrients.
22. Li, J. Q., Rahman, M., Patel, S., Bogner, R. H. & Fan, T. H. Dendritic Morphology and Growth Inhibition of Ice Crystals in Sucrose Solutions. *Cryst. Growth Des.* **22**, 6917–6927 (2022).
23. Gonda, T. & Sei, T. The inhibitory growth mechanism of saccharides on the growth of ice crystals from aqueous solutions. *Prog. Cryst. Growth Charact. Mater.* **51**, 70–80 (2005).
24. Langer, J. S. Instabilities and pattern formation in crystal growth. *Rev. Mod. Phys.* **52**, 1–28 (1980).
25. Cascajo-Castresana, M., David, R. O., Iriarte-Alonso, M. A., Bittner, A. M. & Marcolli, C. Protein aggregates nucleate ice: The example of apoferritin. *Atmos. Chem. Phys.* **20**, 3291–3315 (2020).
26. Melillo, J. H., Nikulina, E., Iriarte-Alonso, M. A., Cerveny, S. & Bittner, A. M. Electron microscopy and calorimetry of proteins in supercooled water. *Sci. Rep.* **12**, 1–11 (2022).

27. Harrison, P. M. & Arosio, P. The ferritins: Molecular properties, iron storage function and cellular regulation. *Biochim. Biophys. Acta - Bioenerg.* **1275**, 161–203 (1996).
28. USDA. FoodData Central. https://fdc.nal.usda.gov/.